SO_2 on $TiO_2(110)$ and $Ti_2O_3(10\bar{1}2)$ Nonpolar Surfaces: A DFT Study

Maurizio Casarin,*,† Francesca Ferrigato,† Chiara Maccato,† and Andrea Vittadini‡

Dipartimento di Scienze Chimiche, Università di Padova, and Istituto di Scienze e Tecnologie Molecolari, C.N.R. di Padova, Padova, Italy

Received: January 18, 2005; In Final Form: April 29, 2005

Density functional molecular cluster calculations have been used to investigate the interaction of SO_2 with defect-free $TiO_2(110)$ and $Ti_2O_3(10\bar{1}2)$ surfaces. Adsorbate geometries and chemisorption enthalpies have been computed and discussed. Several local minima have been found for $TiO_2(110)$, but only one seems to be relevant for the catalytic conversion of SO_2 to S. In agreement with experiment, the bonding of SO_2 to $Ti_2O_3(10\bar{1}2)$ is much stronger than that on $TiO_2(110)$. Moreover, our results are consistent with the surface oxidation and the formation of strong Ti−O and Ti−S bonds. On both substrates, the bonding is characterized by a two-way electron flow involving a donation from the SO_2 HOMO into virtual orbitals of surface Lewis acid sites (L_s^a), assisted by a back-donation from surface states into the SO_2 LUMO. However, the localization of surface states and the strength of back-donation are very different on the two surfaces. On $TiO_2(110)$, back-donation is weaker, and it involves unsaturated bridging O atoms, while on $Ti_2O_3(10\bar{1}2)$, it implies the L_s^a-based valence band maximum and significantly weakens the S−O bond.

1. Introduction

TiO_2 and Ti_2O_3 are probably the best-known among titanium oxides. In contrast to TiO_2, Ti_2O_3 is of little importance for catalytic applications. Nevertheless, the peculiar $3d^1$ electronic configuration of its Lewis acid sites (L_s^a) makes it appealing from a fundamental point of view, because it allows one to study the role played by partially occupied 3d atomic orbitals (AOs) in chemisorption.[1]

The investigation of the interaction of SO_2 with TiO_2 is particularly important, because this material is active in the sulfur recovery from natural, refinery, or coal gasification gases through the $H_2S + SO_2$ Claus reaction.[2,3] Despite the fact that the interaction of SO_2 with rutile $TiO_2(110)$ has been extensively investigated from an experimental point of view,[4] the nature of the surface complexes is not yet completely clear.[5] Moreover, the few theoretical contributions[5,6] so far devoted to this argument have been mainly focused on the adsorption energetics rather than on the analysis of the adsorbate−substrate bonding scheme. In this regard, we know that, on the defect-free surface, SO_2 can be weakly bound both to L_s^a and to Lewis base sites (the bridging oxygen atoms, hereafter L_s^b), to give rise to SO_2 and SO_3-like surface complexes.

As far as the adsorption on Ti_2O_3 is concerned, the only paper so far dedicated to this topic[7] indicates a completely different behavior: SO_2 reacts vigorously with Ti_2O_3, its adsorption is dissociative in character, and it catalyzes the complete oxidation of the surface to TiO_2 and TiS_2.

In our systematic study of the surface chemistry of metal oxides with molecular cluster models and density functional theory (DFT), we already investigated the interaction of a sulfur-containing molecule (H_2S) with rutile $TiO_2(110)$[8] and $Ti_2O_3(10\bar{1}2)$.[9] In the present contribution, we extend our study to the adsorption of SO_2.

* To whom correspondence should be addressed. Phone/fax number ++39-049-8275164/8275161; E-mail maurizio.casarin@unipd.it.
† Dipartimento di Scienze Chimiche, Università di Padova.
‡ Istituto di Scienze e Tecnologie Molecolari, C.N.R. di Padova.

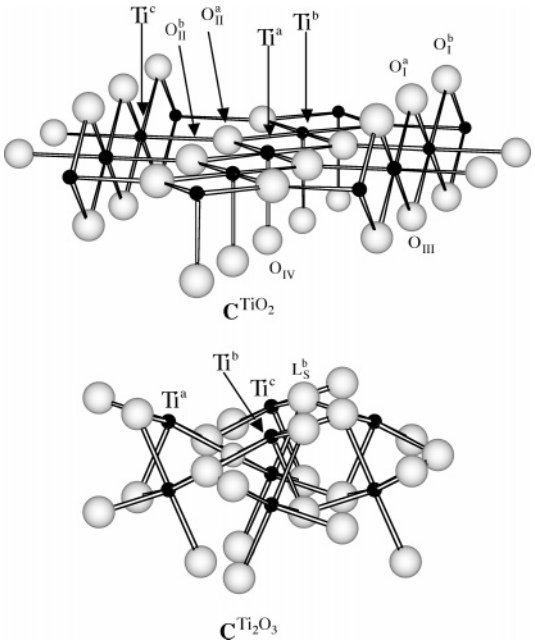

Figure 1. Schematic representation of the employed clusters $\mathbf{C}^{TiO_2}$ and $\mathbf{C}^{Ti_2O_3}$. Saturators are not displayed for the sake of clarity.

2. Computational Details

Defect-free $TiO_2(110)$ has been modeled with a $Ti_{13}O_{29}$ saturated cluster ($\mathbf{C}^{TiO_2}$, see Figure 1) centered on a five-fold-coordinated L_s^a surface ion. $\mathbf{C}^{TiO_2}$ is larger than the cluster adopted by some of us in ref 8 (Ti_7O_9) to model the chemisorption of CO, H_2O, and H_2S on rutile $TiO_2(110)$. This gives the opportunity of employing the same cluster to explore different coordinative modes. At variance to that, $Ti_2O_3(10\bar{1}2)$ has been mimicked by using the same Ti_8O_{24} cluster ($\mathbf{C}^{Ti_2O_3}$, see Figure 1) already employed to investigate the chemisorption of CO, H_2O, and H_2S.[3,9] The experimental lattice constants ($a^{TiO_2} = b^{TiO_2} = 4.587$ Å, $c^{TiO_2} = 2.594$ Å;[10a] $a^{Ti_2O_3} = b^{Ti_2O_3} = 4.7570$ Å, $c^{Ti_2O_3} = 12.9877$ Å[10b]) have been used for both systems.

10.1021/jp050314e CCC: $30.25
Published on Web 06/02/2005

Spurious surface states associated to dangling bonds (DBs) of not chemically complete titanium and oxygen cluster atoms have been eliminated by saturating them with pseudo-hydrogen/hydrogen atoms placed along the bond directions of the extended lattices. In this regard, it deserves to be mentioned that we avoided the embedding of the nonsaturated cluster in a point-charge (PC) array for several reasons. Among them, we emphasize that choosing the "best" values for PCs is almost a matter of taste: Typically adopted values range from the Mulliken charges to the substantially higher formal oxidation numbers. Moreover, in our previous study of the chemisorption of CO, H_2O, and H_2S on TiO_2(110), we showed[8] that the negative effects due to the introduction of the Madelung field through the PC array are much heavier than those introduced by neglecting the field in the model adopting the pseudo-hydrogen saturators.

All the molecular cluster calculations have been run within DFT by using the *ADF 2002* package.[11] Optimized geometries and chemisorption enthalpies have been evaluated by employing generalized gradient corrections self-consistently included through the Becke−Perdew formula.[12] A triple-ζ Slater-type basis set has been used for Ti and adsorbate atoms, while a double-ζ basis set has been adopted for the host O atoms as well as for saturators. Inner cores of Ti (1s2s2p), S (1s2s2p), and O (1s) atoms have been treated by the frozen-core approximation.

The adsorption enthalpy (ΔH) has been analyzed in terms of adsorbate and substrate fragment orbitals through the use of the Ziegler's extended transition-state method[13]

$$\Delta H = \Delta E_{\text{elstat}} + \Delta E_{\text{Pauli}} + \Delta E_{\text{int}} + \Delta E_{\text{prep}}$$

where ΔE_{elstat} is the pure electrostatic interaction, ΔE_{Pauli} is the destabilizing two-orbital-four-electron interaction between the occupied orbitals of the two interacting fragments ($\Delta E_{\text{elstat}} + \Delta E_{\text{pauli}} = \Delta E_{\text{steric}}$), ΔE_{int} derives from the stabilizing interaction between occupied and empty orbitals of the fragments, and the last term, ΔE_{prep}, is the energy required to relax the structure of the free fragments to the geometry of the final system. Adsorption enthalpies have been further corrected by taking into account the basis set superposition error (BSSE), which was estimated through the use of reference energies computed with ghost adsorbate and surface fragments.[14]

Information about the localization and the bonding/antibonding character of molecular orbitals (MOs) over a broad range of energies has been obtained by referring to density of states (DOS), partial DOS (PDOS), and crystal orbital overlap population (COOP) curves. These have been computed by weighting one-electron energy levels by their basis orbital percentage and by applying a 0.25 eV Lorentzian broadening.

3. Results and Discussion

We first checked the capability of $\mathbf{C}^{TiO_2}$ of reproducing the structural relaxation undergone by TiO_2(110). For this purpose, we optimized the coordinates of Ti^a, Ti^b, Ti^c, O_I^a, O_I^b, and O_{II} (the atom labeling is reported in Figure 1) with the constraint of maintaining the C_{2v} symmetry of $\mathbf{C}^{TiO_2}$. The obtained displacements compare quite well with literature experimental[15] and theoretical values;[8,16] moreover, the main features of the electronic structure of $\mathbf{C}^{TiO_2}$ are very similar to those obtained for the smaller Ti_7O_9 cluster we adopted in ref 8.[17,18]

3.1. The SO_2 Free Molecule. Understanding the adsorption of SO_2 requires a detailed knowledge of its electronic structure. We briefly summarize the results obtained by running DFT calculations on the isolated molecule (see Table 1). Symmetry properties of the closed-shell SO_2 are described by the C_{2v} symmetry point group.[20] Its valence manifold (see Figure 2) includes a total of seven molecular orbitals MOs ((inner) $1b_1^2 2b_2^2 3a_1^2 1a_2^2 3b_2^2 4a_1^2/2b_1^0$). Among them, both the $4a_1$ HOMO and the $2b_1$ LUMO[21] are antibonding in nature (see COOPs in Figures 2 and 3-D contour plots in Figure 3), even though the latter accounts for a stronger S−O repulsive interaction. Symmetry and overlap considerations suggest that SO_2 frontier orbitals will be the most perturbed upon chemisorption. However, as a consequence of their antibonding nature, the participation of the HOMO (LUMO) to the $SO_2 \rightarrow$ substrate (substrate $\rightarrow SO_2$) donation will strengthen (weaken) the S−O bond.

TABLE 1: Selected Molecular Properties of the SO_2 Molecule: Bond Length (BL), Bond Angle (BA), Dipole Moment (μ), Ionization Potential (IP), Binding Energy (BE), Vibrational Frequency (ν)

	theor	exptl
r_{S-O} (Å)	1.465	1.432[a]
O−Ŝ−O (°)	120.3	119.32[a]
μ (D)	1.62	1.60[b]
IP_{4a1}	12.23	12.5[c]
IP_{3b2}	12.99	13.5[c]
IP_{1a2}	13.53	13.2[c]
ν_1 (cm^{-1})	1095.0	1151.4[d]
ν_2 (cm^{-1})	477.8	517.8[d]
ν_3 (cm^{-1})	1297.1	1360[d]
BE (kcal/mol)	290.25	254.4[e]
Q_M^S	1.04[f]	
Q_M^O	−0.52[f]	
Q_H^S	0.42[f]	
Q_H^O	−0.21[f]	

[a] ref 23. [b] ref 24. [c] ref 25. [d] ref 26. [e] ref 27. [f] Q_M^X and Q_H^X stand for Mulliken[28] and Hirschfeld[29] atomic charges.

3.2. SO_2 on the Defect-Free TiO_2(110) Surface. The interaction of SO_2 with TiO_2(110) has been modeled by considering the different coordinative modes reported in Figure 4. Structures were optimized within the highest possible symmetries, that is, C_{2v} for SO_2 atop Ti^a (a_1 and a_2), C_s for the SO_3-like and μ-SO_2 geometry, and C_1 for the μ-SO_3 and η^1-SO_3 coordination.

In Table 2, selected structural parameters, chemisorption enthalpies, and Hirschfeld/Mulliken atomic charges are reported, while different contributions to chemisorption enthalpy are displayed in Table 3. Data pertaining to the a_1-SO_2 geometry have not been included in the table, because this surface complex is computed to be highly unstable as a consequence of the strong repulsive interaction between the adsorbate O lone pairs (n) and O_{II}-based surface states. As a whole, the outcomes of our calculations indicate that the SO_2−TiO_2(110) interaction is quite weak, almost negligible for the SO_3-like and μ-SO_3 coordinations and a little stronger for the μ-SO_2 and η^1-SO_3 arrangements. These results agree very well with supercell DFT calculations recently carried out by Zhang and Lindan (ZL);[5] moreover, it is noteworthy that our evaluation of the chemisorption enthalpy for the most stable arrangements (μ-SO_2 and η^1-SO_3) agrees quantitatively with those reported by ZL (−9.92 and −11.30 kcal/mol, respectively) for the same arrangements. Interestingly, despite the similarity of $\Delta H^{\mu-SO_2}$ and $\Delta H^{\eta^1-SO_3}$, the two surface complexes seem to imply different bonding schemes. In fact, even though SO_2 behaves as an electron donor in both cases,[30] donation and back-donation mechanisms appear to compensate each other when the η^1-SO_3 complex is formed (see Table 2). In this regard, the information provided by data reported in Table 3 is particularly interesting. Among the

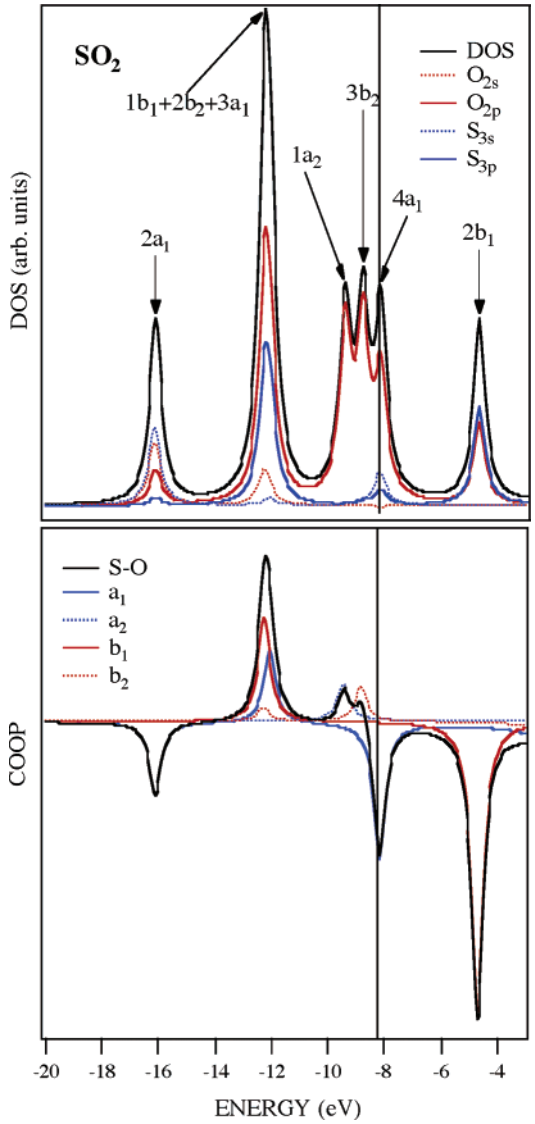

Figure 2. DOS (top) and corresponding COOPs (bottom) of the free SO_2 molecule. Vertical bars represent the HOMO energy.

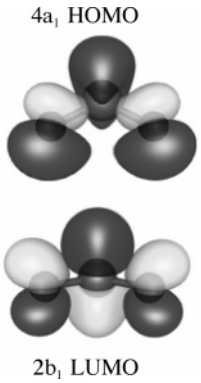

Figure 3. 3-D plots of the $4a_1/2b_1$ HOMO/LUMO of the free SO_2. Dark and light surfaces correspond to the wave function values of 0.04 $e^{1/2}/Å^{3/2}$ and -0.04 $e^{1/2}/Å^{3/2}$, respectively.

coordinative modes we considered, those characterized by the strongest covalent interaction are the μ-SO_3 and η^1-SO_3 ones. On the other hand, ΔE_{steric} and ΔE_{prep} corresponding to these geometries are also very high, and the final ΔH is the result of a balance of different contributions. Moving to μ-SO_2, we already mentioned that $\Delta H^{\mu-SO_2}$ and $\Delta H^{\eta^1-SO_3}$ are very similar. On the other hand, data reported in Table 3 clearly indicate

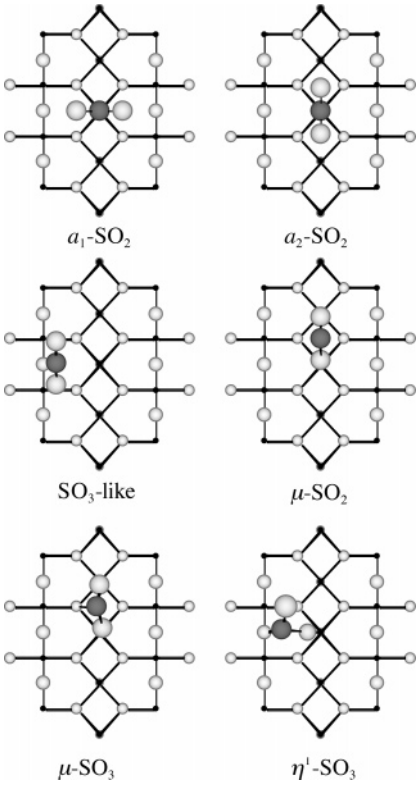

Figure 4. Schematic representation (top view) of the coordinative arrangements we explored for SO_2 on the defect-free TiO_2(110).

TABLE 2: Selected Structural Parameters of TiO_2(110)$-SO_2$ Surface Complexes. Adsorption Enthalpies and $Q_H^{SO_2}/Q_M^{SO_2}$ Charges Are Also Included

	a_2-SO_2	SO_3-like	μ-SO_2	μ-SO_3	η^1-SO_3
r_{S-O^1} (Å)[b]	1.463	1.470	1.471	1.490	1.528
r_{S-O^2} (Å)	1.463	1.471	1.479	1.509	1.464
r_{Ti^a-S} (Å)	3.537				
$r_{Ti^a-O^1}$ (Å)			2.526	2.374	2.142
$r_{Ti^b-O^2}$ (Å)			2.418	2.280	
$r_{O_I^a-S}$ (Å)		2.830		2.185	2.163
OŜO (°)	120.4	118.0	119.2	115.0	112.6
$Q_H^{SO_2}/Q_M^{SO_2}$			0.38 (0.16)		0.14 (−0.05)
ΔH (kcal/mol)	0.06	−3.46	−9.53	−2.72	−10.98

[b] The O^1 corresponds to the SO_2 O-atom bonded to the L_s^a.

TABLE 3: Theoretical Adsorption Enthalpies (kcal/mol) Pertaining to SO_2 on TiO_2(110) Decomposed by Means of the Ziegler Transition-State Method

	a_2-SO_2	SO_3-like	μ-SO_2	μ-SO_3	η^1-SO_3
ΔE_{steric}	2.69	1.14	6.49	59.85	48.57
ΔE_{inter}	−4.13	−5.79	−19.74	−73.06	−75.96
$\Delta E_{prep}^{cluster}$	0.07	0.14	1.48	5.74	10.61
$\Delta E_{prep}^{SO_2}$	0.01	0.08	0.11	1.92	3.57
$BSSE^{cluster}$	0.87	0.61	1.57	1.97	1.50
$BSSE^{SO_2}$	0.55	0.36	0.56	0.86	0.73
ΔH	0.06	−3.46	−9.53	−2.72	−10.98

that this is not due to a particularly strong covalent interaction between the substrate and the SO_2 molecule symmetrically bridging two surface L_s^a, but rather, it is a consequence of the low ΔE_{steric} and ΔE_{prep} values.

Further insights into the μ-SO_2 and η^1-SO_3 bonding schemes can be gained by referring to Figures 5 and 6. In the former, the SO_2 PDOS and S−O COOPs for both coordinations are compared with corresponding DOS and COOPs of the free molecule, while in the latter, Ti^a-SO_2, O_I-SO_2, and $O_{II}-SO_2$

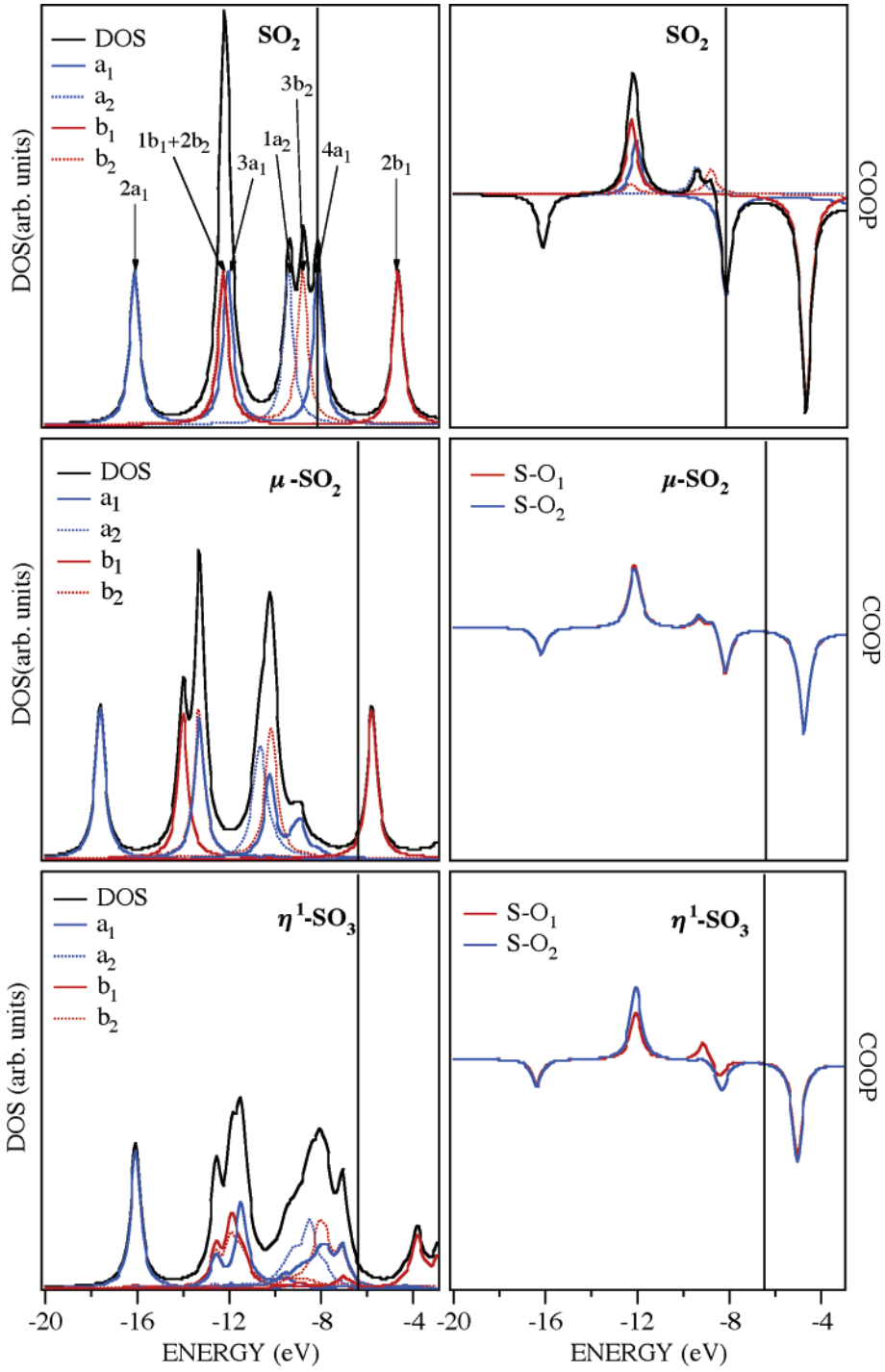

Figure 5. SO_2 PDOS and S−O COOPs corresponding to the μ-SO_2 and η^1−SO_3 coordinative modes on the perfect TiO_2(110) surface. Data pertaining to the free adsorbate are also included for comparison. Vertical bars represent the HOMO energy.

COOPs are displayed. The inspection of Figure 5 reveals that the SO_2 electronic structure is significantly perturbed upon chemisorption, independently of the surface complex geometry. More specifically, the MOs reminiscent of the SO_2 $4a_1$, $3b_2$, and $1a_2$ levels are stabilized (destabilized) for the μ-SO_2 (η^1-SO_3) arrangement.[31] Moreover, Figure 6 testifies that the μ-SO_2 surface complex is characterized by an extensive charge transfer from the SO_2 HOMO (the weakly S−O antibonding $4a_1$ level) into L_s^a 3d and 4p virtual orbitals (L_s^a 4s AOs participate to a negligible extent) and by the absence of any substrate → SO_2 back-donation.[32]

The bonding picture of the η^1-SO_3 surface complex is more involved. The adsorbate−substrate interaction consists of a two-way electron flow implying a donation from the SO_2 outermost MOs into L_s^a virtual orbitals (again 3d and 4p AOs) assisted by a multicentered substrate → SO_2 back-donation involving a charge transfer from both the $n^{O_1^a}$ (parallel to the surface) and the $DB^{O_1^a}$ (perpendicular to the surface) into the SO_2 $2b_1$ LUMO (see Figure 6). The significant participation of the SO_2-based $2b_1$ level (strongly S−O antibonding in nature) to the adsorbate−substrate interaction provides a rationale of the different electronic and structural perturbations undergone by the adsorbate upon chemisorption. In this regard, it is noteworthy that the weakening of a S−O bond, a necessary step of the catalytic conversion of SO_2 to S,[2] is favored only by the η^1-SO_3 arrangement.

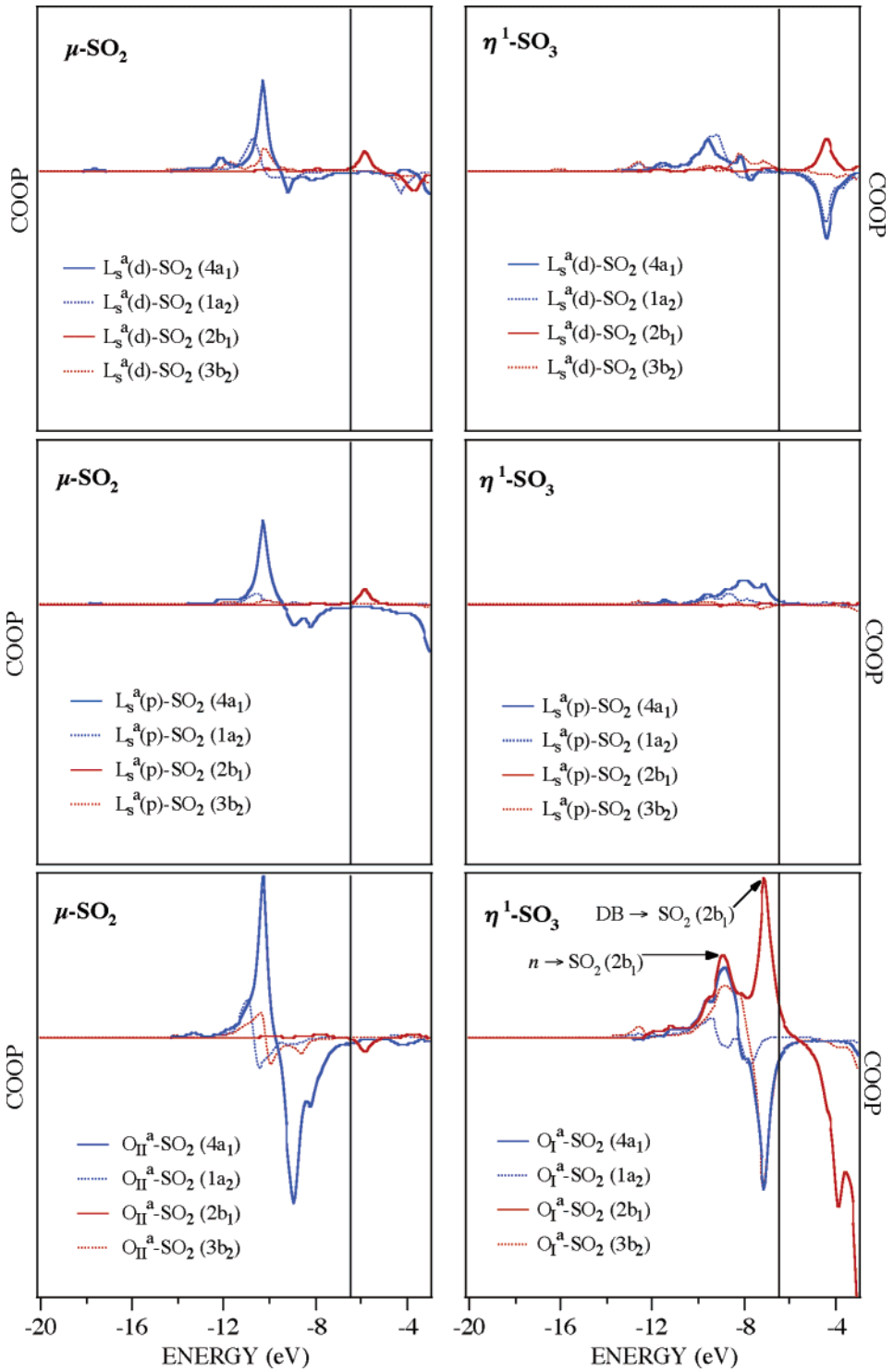

Figure 6. Ti^a-SO_2, O_I-SO_2, and $O_{II}-SO_2$ COOPs. The $4s^{Ti^a}-SO_2$ has not been included because it is negligible. Vertical bars represent the HOMO energy.

The analysis of the surface atomic displacements indicate that the strongest structural perturbations are pertinent to the η^1-SO_3 geometry and that they are not limited to the atoms (Ti^a, O_1^a) directly involved in the adsorbate−substrate interaction.

As a whole, the obtained results compare quite well with experimental evidence indicating a molecular adsorption of SO_2 on nearly perfect TiO_2(110) at low temperature through the involvement of surface L_s^a and L_s^b.[4c]

3.3. SO_2 on the Defect-Free $Ti_2O_3(10\bar{1}2)$ Surface. The interaction of SO_2 with the defect-free $Ti_2O_3(10\bar{1}2)$ surface has been modeled by considering three coordination geometries (see Figure 7) and limiting the optimization procedure to the coordinates of the adsorbate atoms.[3,9,33,34]

In Table 4, selected structural parameters, chemisorption enthalpies, and Q_H/Q_M values are reported, while different contributions to chemisorption enthalpy are included in Table 5. Data pertaining to the η^1-SO_2 starting coordination is missing, because it does not correspond to a local minimum. Theoretical results clearly indicate that, in agreement with experiment, the SO_2−substrate interaction is very different for TiO_2(110)[4] and $Ti_2O_3(10\bar{1}2)$[7] surfaces. In detail, (i) independently of the surface complex geometry, SO_2 behaves as net electron acceptor (see

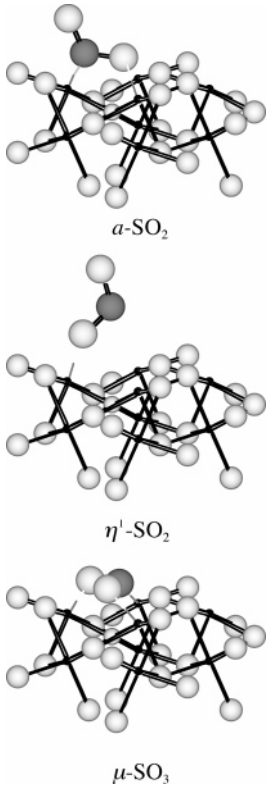

Figure 7. Schematic representation of the coordinative modes we explored for SO_2 on the defect-free $Ti_2O_3(10\bar{1}2)$.

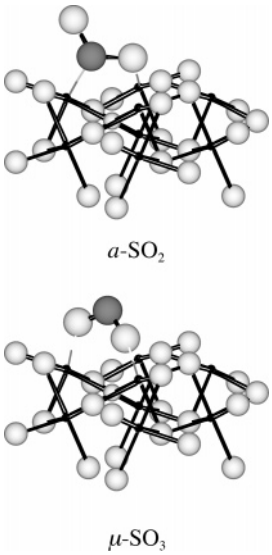

Figure 8. Schematic representation of the optimized a-SO_2 and μ-SO_2 coordinative modes on the unrelaxed $Ti_2O_3(10\bar{1}2)$.

Table 4), (ii) the S−O bond lengths are dramatically lengthened upon chemisorption, (iii) L_s^a−O^{SO_2} internuclear distances range between 1.924 and 1.982 Å (i.e., they are computed shorter than those of the Ti_2O_3 bulk phase (2.0681 and 2.0245 Å)[10b] and very close to those pertaining to TiO_2 (1.949 and 1.969 Å)),[10a] (iv) L_s^a−S internuclear distance computed for the most stable arrangement (μ-SO_3) is 2.677 Å, a value slightly longer than the actual Ti−S bond lengths in the TiS_2 bulk phase (2.429 Å)[35] and in other nonstoichiometric titanium sulfides (2.332−2.544 Å),[36−38] and (v) the large ΔH values and the corresponding ΔE_{inter} and ΔE_{prep} contributions are indicative of an incipient S−O bond breaking and of Ti−O and Ti−S bond formation. Interestingly, as already found for CO, H_2O, and H_2S on the same surface, the adsorbate−substrate interaction is dominated by covalent interactions (see Table 5) and, more specifically, by back-donation from the Ti_2O_3 VBM into the $2b_1$ SO_2 LUMO (see Figure 9). Such a participation of the Ti_2O_3 VBM to the adsorbate−substrate interaction will certainly affect structural and electronic properties of the surface; on the other hand, any attempt to look into these perturbations is hampered by our frozen substrate approximation.[39]

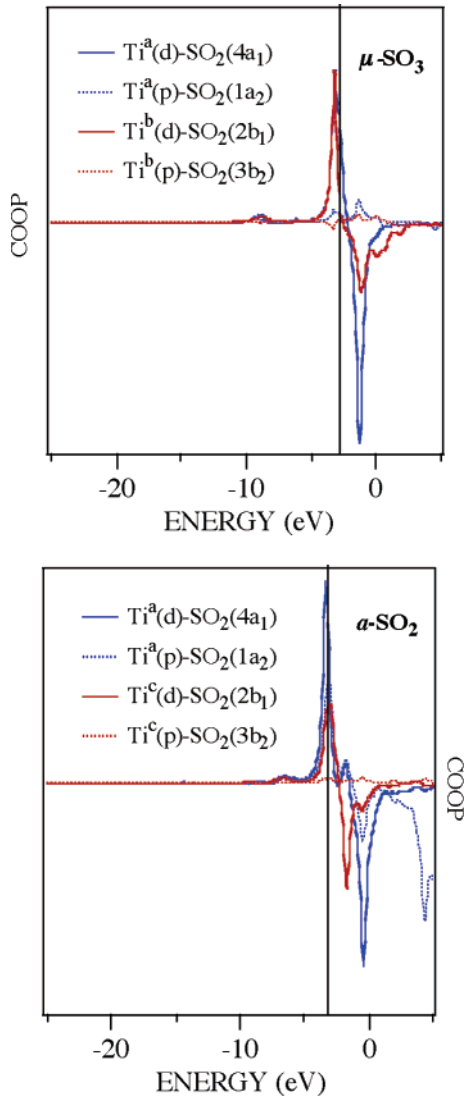

Figure 9. Ti^a−SO_2, Ti^b−SO_2, and Ti^c−SO_2, COOPs. Contributions from Ti-based 4s AOs have not been included because they are negligible. Vertical bars represent the HOMO energy.

TABLE 4: Selected Bond Lengths (Å) and Bond Angles (°) of $Ti_2O_3(10\bar{1}2)$−SO_2 Surface Complexes. Adsorption Enthalpies (kcal/mol) and Charges Are Also Included[a]

	a-SO_2	μ-SO_3
r_{S-O^1}	1.604	1.608
r_{S-O^2}	1.504	1.610
r_{Ti^c-S}	2.677	
$r_{Ti^c-O^1}$		1.924
$r_{Ti^c-O^2}$		1.952
$r_{Ti^c-O^1}$	1.982	
$\hat{OSO}$	112.5	110.0
$Q_M^{SO_2}$	−0.18	−0.24
$Q_H^{SO_2}$	−0.47	−0.82
ΔH (kcal/mol)	−40.18	−63.45

[a] Atom labeling is reported in Figure 1.

TABLE 5: Theoretical Adsorption Enthalpies (kcal/mol) Pertaining to SO_2 on $Ti_2O_3(10\bar{1}2)$ Decomposed by Means of the Ziegler Transition-State Method

	a-SO_2	μ-SO_3
ΔE_{steric}	52.80	68.22
ΔE_{inter}	−105.88	−154.86
$\Delta E_{prep}^{cluster}$		
$\Delta E_{prep}^{SO_2}$	11.04	21.02
$BSSE^{cluster}$	1.07	1.36
$BSSE^{SO_2}$	0.79	0.81
ΔH	−40.18	−63.45

Despite their semiquantitative nature, theoretical results herein reported for SO_2 on $Ti_2O_3(10\bar{1}2)$ testify to the crucial role played by the L_s^a 3d electrons in chemisorption processes taking place on transition-metal oxide surfaces. This evidence confirms that, as pointed out by Barteau,[40] metal cations exposed at the surface of metal oxides have much in common with their counterparts in solution.

4. Conclusion

Theoretical results herein reported demonstrate that small saturated clusters are able to predict the behavior of SO_2 on the clean, defect-free $TiO_2(110)$ surface. According to experiment and other theoretical outcomes, the adsorption is found to be molecular in nature and characterized by a small ΔH (∼10 kcal/mol). The most stable arrangements correspond to the μ-SO_2 and η^1-SO_3 species, whose electronic structure is however very different. Interestingly, the latter surface complex could be of some relevance in the catalytic conversion of SO_2 to S. As far as the chemisorption of SO_2 on the $Ti_2O_3(10\bar{1}2)$ surface, our results agree with experimental data in predicting a definitely stronger adsorbate−substrate interaction. Moreover, theoretical outcomes indicate that such an interaction is dominated by the back-donation from the L_s^a-based VBM into the SO_2 $2b_1$ LUMO.

References and Notes

(1) (a) Casarin, M.; Maccato, C.; Vittadini, A. *J. Phys. Chem. B* **2002**, *106*, 795. (b) Casarin, M.; Nardi, M.; Vittadini, A. *Surf. Sci.* **2004**, *566*−*568P1*, 451.

(2) Pièplu, A.; Saur, O.; Lavalley, J.-C.; Legendre, O.; Nédez, C. *Catal. Rev.*—*Sci. Eng.* **1998**, *40*, 409.

(3) Diebold, U. *Surf. Sci. Rep.* **2003**, *48*, 53.

(4) (a) Smith, K. E.; Mackay, J. L.; Henrich, V. E. *Phys. Rev. B* **1987**, *35*, 5822. (b) Onishi, H.; Aruga, T.; Egawa, C.; Iwasawa, Y. *Surf. Sci.* **1988**, *193*, 33. (c) Warburton, D. R.; Purdie, D.; Muryn, C. A.; Prabhakaran, K.; Wincott, P. L.; Thornton, G. *Surf. Sci.* **1992**, *270*, 305. (d) Sayago, D. I.; Serrano, P.; Böhme, O.; Goldoni, A.; Paolucci, G.; Roman, E.; Martın-Gago, J. A. *Phys. Rev. B* **2001**, *64*, 205402. (e) Sayago, D. I.; Serrano, P.; Böhme, O.; Goldoni, A.; Paolucci, G.; Roman, E.; Martın-Gago, J. A. *Surf. Sci.* **2001**, *482*, 9.

(5) Zhang, C.; Lindan, P. J. D. *Chem. Phys. Lett.* **2003**, *373*, 15.

(6) Rodriguez, J. A.; Liu, G.; Jirsak, T.; Hrbek, J.; Chang, Z.; Dvorak, J.; Maiti, A. *J. Am. Chem. Soc.* **2002**, *124*, 5242.

(7) Smith, K. E.; Henrich, V. E. *Phys. Rev. B* **1985**, *32*, 5384.

(8) (a) Casarin, M.; Maccato, C.; Vittadini, A. *J. Phys. Chem. B* **1998**, *102*, 10745. (b) Casarin, M.; Maccato, C.; Vittadini, A. *J. Phys. Chem. B* **1999**, *103*, 3510. (c) Casarin, M.; Maccato, C.; Vittadini, A. *Appl. Surf. Sci.* **1999**, *142*, 196.

(9) Casarin, M.; Vittadini, A. *Phys. Chem. Chem. Phys.* **2003**, *5*, 2461.

(10) (a) Howard, C. J.; Sabine, T. M.; Dickson, F. *Acta Crystallogr., Sect. B* **1991**, *47*, 462. (b) Rice, C. E.; Robinson, W. R. *Acta Crystallogr., Sect. B* **1977**, *33*, 1342.

(11) *Amsterdam Density Functional Package*, version 2002; Vrjie Universiteit: Amsterdam, The Netherlands, 2002.

(12) (a) Becke, A. D. *Phys. Rev. A* **1988**, *38*, 3098. (b) Perdew, J. P. *Phys. Rev. B* **1986**, *33*, 8822.

(13) Ziegler, T.; Rauk, A. *Theor. Chim. Acta* **1977**, *46*, 1.

(14) Rosa, A.; Ehlers, A. W.; Baerends, E. J.; Snijders, J. G.; te Velde, G. *J. Phys. Chem.* **1996**, *100*, 5690.

(15) Charlton, G.; Howes, P. B.; Nicklin, C. L.; Steadman, P.; Taylor, J. S. G.; Muryn, C. A.; Harte, S. P.; Mercer, J.; McGrath, R.; Norman, D.; Turner, T. S.; Thornton, G. *Phys. Rev. Lett.* **1997**, *78*, 495.

(16) (a) Ramamoorthy, M.; Vanderbilt, D.; King-Smith, R. D. *Phys. Rev. B* **1994**, *49*, 16721. (b) Vogtenhuber, D.; Podloucky, R.; Neckel, A.; Steinemann, S. G.; Freeman, A. J. *Phys. Rev. B* **1994**, *49*, 2099. (c) Reinhardt, P.; Hess, B. A. *Phys. Rev. B* **1994**, *50*, 12015. (d) Bates, S. P.; Kresse, G.; Gillan, M. J. *Surf. Sci.* **1997**, *385*, 386.

(17) As far as the $TiO_2(110)$ electronic structure is concerned, we point out that the valence band maximum (VBM) is mainly localized on the surface L_s^b (the bridging oxygen atoms), while the conduction band minimum (CBM) is mainly localized on 3d AOs of surface L_s^a.

(18) Although the electronic structure of $\mathbf{C}^{Ti_2O_3}$ has been thoroughly described in ref 3, it may be useful for the forthcoming discussion to herein summarize its main features. The outermost occupied MOs, representative of the $Ti_2O_3(10\bar{1}2)$ VBM, are grouped in an energy range of 0.2 eV; they are all localized on the d_{z^2} AO of the eight Ti atoms of $\mathbf{C}^{Ti_2O_3}$, and all of them have a Ti−Ti bonding character. The top of the O 2p band lies 2.5 eV below the innermost of the Ti−Ti bonding MOs and, according to the results of the Henrich group,[19] it extends for ∼6 eV. Furthermore, once again in agreement with the ultraviolet photoelectron spectroscopy (UPS) measurements of Smith and Henrich,[19d] the O 2p PDOS is characterized by a double-peaked structure. The higher-energy peak is due to nonbonding MOs (the threshold of the O 2p band is originated by the occupied L_s^b dangling bonds), while the lower-energy one includes the bonding partners.

(19) (a) Kurtz, R. L.; Henrich, V. E. *Phys. Rev. B* **1982**, *25*, 3563. (b) Kurtz, R. L.; Henrich, V. E. *Phys. Rev. B* **1982**, *26*, 6682. (c) McKay, J. M.; Henrich, V. E. *Surf. Sci.* **1984**, *137*, 463. (d) Smith, K. E.; Henrich, V. E. *Phys. Rev. B* **1988**, *38*, 5965. (e) Smith, K. E.; Henrich, V. E. *Phys. Rev. B* **1988**, *38*, 9571. (f) Smith, K. E.; Henrich, V. E. *J. Vac. Sci. Technol., A* **1989**, *7*, 1967. (g) Kurtz, R. L.; Henrich, V. E. *Surf. Sci. Spectra* **1998**, *5*, 182.

(20) Herzberg, G. *Electronic Spectra of Polyatomic Molecules*; Van Nostrand Reinhold Company: New York, 1966.

(21) Despite the general agreement between theory and experiment, our calculations fail in predicting the correct order of the closely spaced ionization potentials of $1a_2$ and $3b_2$ MOs (see Table 1). On the other hand, it is well-known that MOs playing a leading role in determining the reactivity of a molecular system are the highest occupied MO (HOMO) and the lowest unoccupied MO (LUMO), collectively indicated as frontier orbitals.[22]

(22) Miessler, G. L.; Tarr, D. A. *Inorganic Chemistry*; Prentice Hall: Upper Saddle River, NJ, 1998.

(23) Kivelson, D. *J. Chem. Phys.* **1954**, *22*, 904.

(24) *Handbook of Chemistry and Physics*, 64th ed. E-92; CRC Press: Boca Raton, FL, 1984.

(25) Turner, D. W.; Baker, C.; Baker, A. D.; Brundle, C. R. *Molecular Photoelectron Spectroscopy*; Wiley: New York, 1970.

(26) Barker, E. F. *Rev. Mod. Phys.* **1942**, *14*, 198.

(27) Huheey, J. E. *Inorganic Chemistry: Principle of Structure and Reactivity*, 2nd ed.; Harper & Row: New York, 1978.

(28) Mulliken, R. S. *J. Chem. Phys.* **1955**, *23*, 1833.

(29) Hirshfeld, F. L. *Theor. Chim. Acta* **1977**, *44*, 129.

(30) In the μ-SO_2/η^1-SO_3 coordinations $Q_H^{Ti^a}$($Q_M^{Ti^a}$) passes from 0.68 (2.02) to 0.60/0.61 (1.93/1.94) upon chemisorption.

(31) On passing from the free SO_2 to μ-SO_2, the shift toward lower energies of $4a_1$, $3b_2$, and $1a_2$ MOs is not uniform. Corresponding $|\Delta E|$'s amount to 2.00, 1.32, and 1.14 eV, respectively.

(32) Internuclear distances between L_s^a and adsorbate O atoms (∼2.46 Å) are quite close to the one we evaluated for H_2O (2.41 Å)[8] on the same surface. Moreover, the slightly different L_s^a−O values reported in Table 2 are due to the symmetry of the corresponding $\mathbf{C}^{TiO_2}$−SO_2 cluster: C_s.

(33) The starting geometries have been labeled as (i) a-SO_2, with the adsorbate bonded to a surface L_s^a through the S atom; (ii) η^1-SO_3, with the adsorbate bonded to a surface L_s^a through one of its O atoms; (iii) μ-SO_3, with the O atoms of the adsorbate positioned a-top two surface L_s^a and the S species interacting with a surface L_s^b.

(34) Periodic DFT calculations are in progress in our laboratory to investigate the clean $Ti_2O_3(10\bar{1}2)$ surface.

(35) Chianelli, R. R.; Scanlon, J. C.; Thompson, A. H. *Mater. Res. Bull.* **1975**, *10*, 1379.

(36) Wadsley, A. D. *Acta Crystallogr.* **1957**, *10*, 715.

(37) Tronc, P. E.; Moret, R.; Legendre, J. J.; Huber, M. *Acta Crystallogr., Sect. B* **1975**, *B31*, 2800.

(38) 2.332 and 2.544 Å are the shortest and longest Ti−S internuclear distances of the nonstoichiometric compound Ti_8O_{12}.[36] In the $Ti_{2+x}S_4$ ($0.2 < x < 1$) phase, the Ti−S BL is 2.45 Å.[37]

(39) We already stressed in ref 3 that, even if $\mathbf{C}^{Ti_2O_3}$ reproduces well the electronic features of the clean $Ti_2O_3(10\bar{1}2)$ surface, it is not well-suited to describe structural relaxation because of its asymmetry and limited size. Any attempt to get self-consistent field (SCF) convergence for larger clusters was not fruitful.[34]

(40) Barteau, M. A. *J. Vac. Sci. Technol.* **1993**, *11*, 2162.